

SUPPORTING INFORMATION

Hierarchically Packed Liquid Epoxy Composites with Ultralow CTE and Viscosity for High-Performance Wafer- Level Packaging

Cheng-Ti Hu,^{1,†} Huai-Shu Yang,^{2,†} Chiao-Yin Yang,¹ Chin-Yu Wu,¹ Po-Hsun Chiu,¹
Chih-Chen Hsieh,¹ Yi-Huan Lee,^{3,*} Chi-Yang Chao,² and Chi-An Dai,^{1,*}

¹Department of Chemical Engineering, ²Department of Materials Science and
Engineering, National Taiwan University, Taipei, 10617, Taiwan

³Department of Molecular Science and Engineering, National Taipei University of
Technology, Taipei, 106344, Taiwan

[†]These authors contributed equally to the work.

*Corresponding authors. E-mail: yihuanlee@ntut.edu.tw (Y.-H. Lee);
polymer@ntu.edu.tw (C.-A. Dai)

ADDITIONAL FIGURES

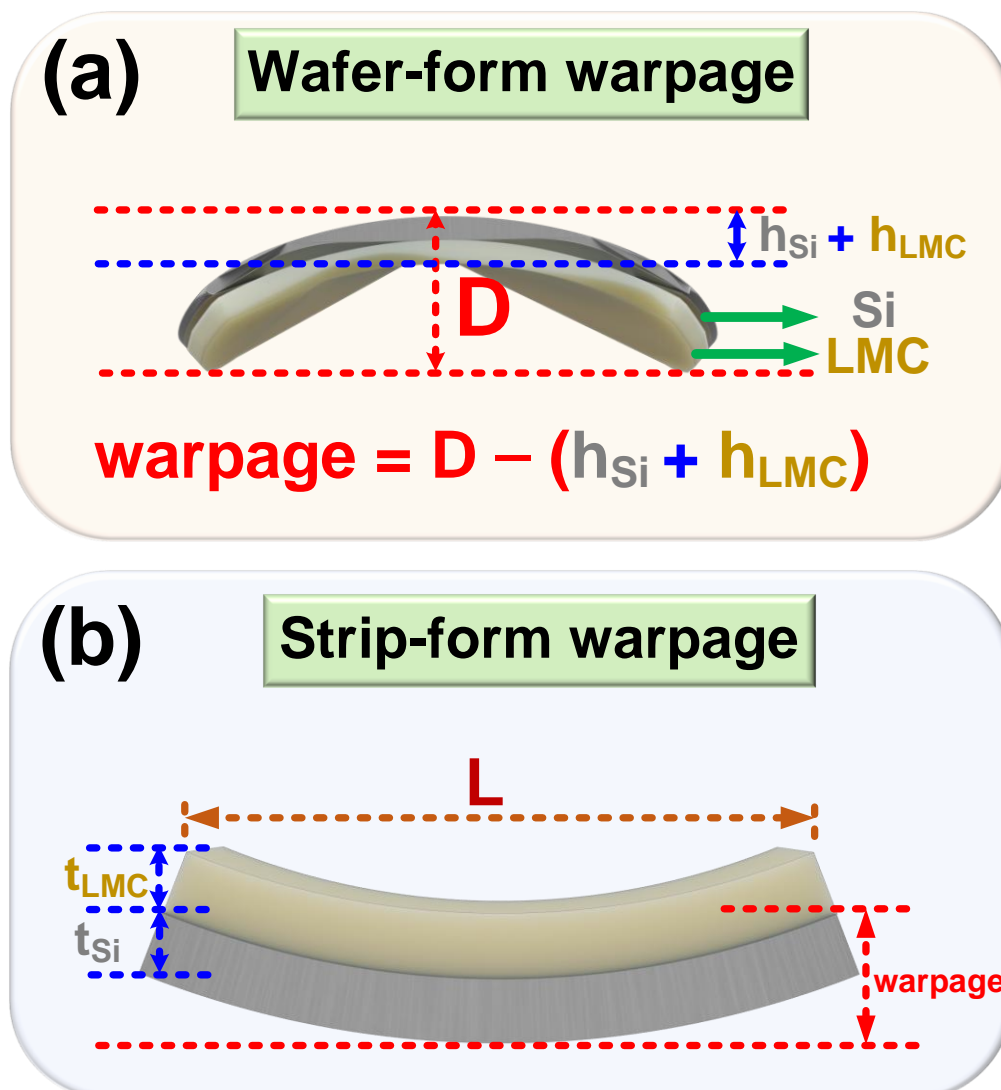


Figure S1. Schematic representation of the warpage definitions in (a) wafer-form and (b) strip-form configurations. In the wafer-form warpage test, the warpage is defined as the difference between the total deflection (D) of the inverted (frown-shaped) structure—with the LMC layer facing downward—and the combined thicknesses of the silicon wafer (h_{Si}) and LMC layer (h_{LMC}). In the strip-form test, the warpage is defined as the vertical height difference between the ends of the silicon strip and the central silicon–LMC interface in a smile-shaped configuration ($\text{warpage} = D - h_{Si} - h_{LMC}$), where the silicon substrate is positioned at the bottom.

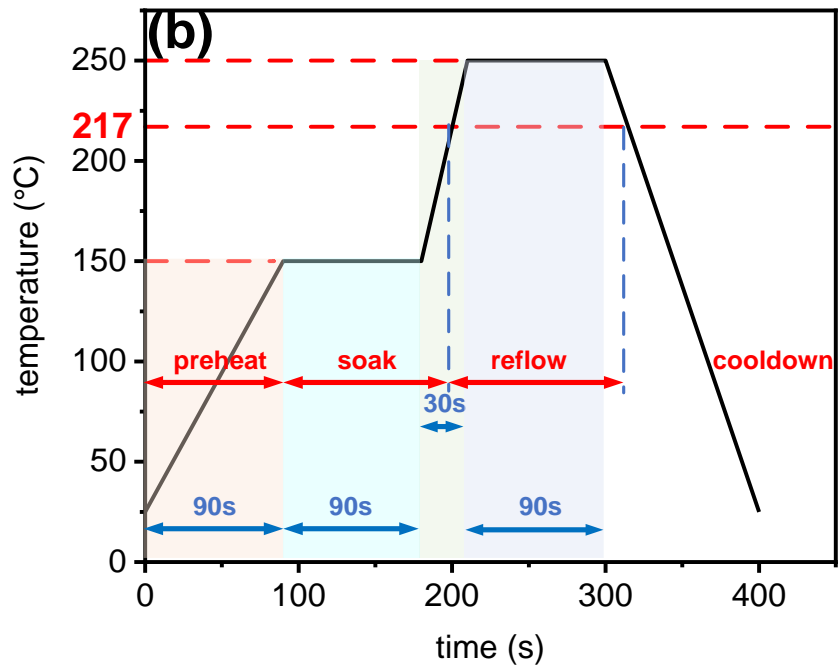
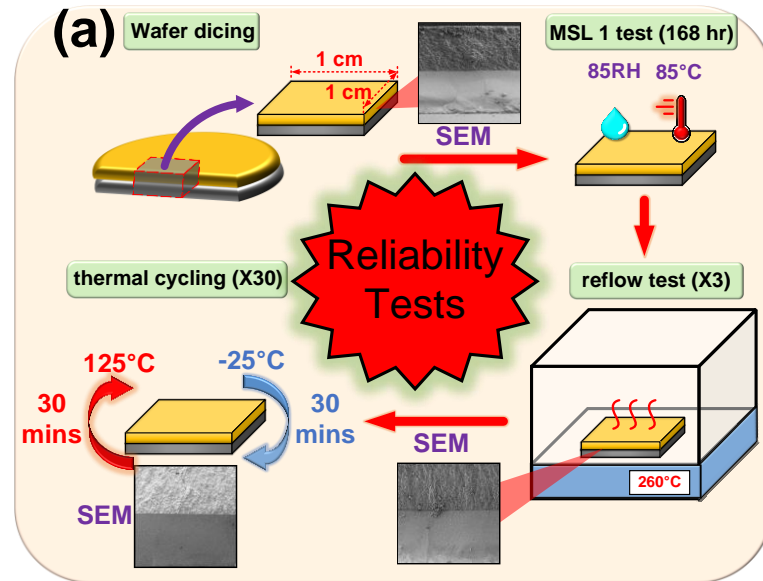


Figure S2. (a) Schematic representation of the molded chip reliability test flow. The molded wafer was diced into rectangular 1 cm × 1 cm chips, followed by sequential exposure to MSL1 conditioning (85 °C, 85% RH for 168 h), three simulated reflow cycles, and a final thermal cycling test consisting of 30 cycles between –25 °C and 125 °C (30 min dwell at each temperature). SEM observations of the LMC/silicon interface were conducted after dicing, after reflow, and after thermal cycling to monitor interfacial changes. (b) Representative temperature profile of the simulated reflow process used in this study.

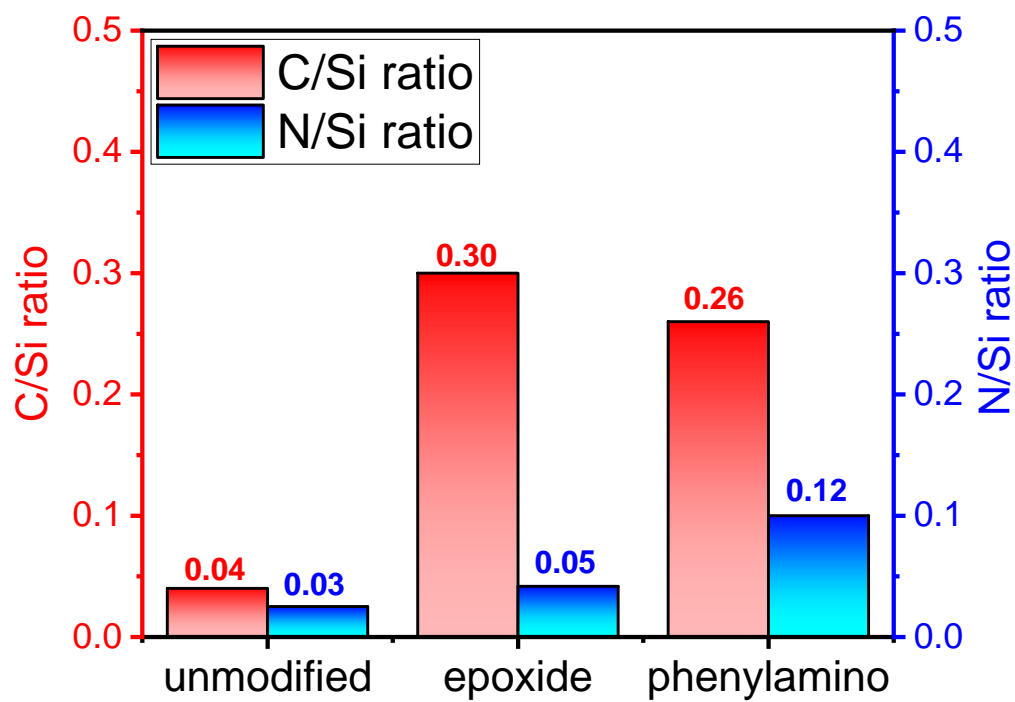


Figure S3. Calculated C/Si and N/Si atomic ratios of unmodified, epoxide-modified, and phenylamino-modified coarse silica obtained from EDS analysis.

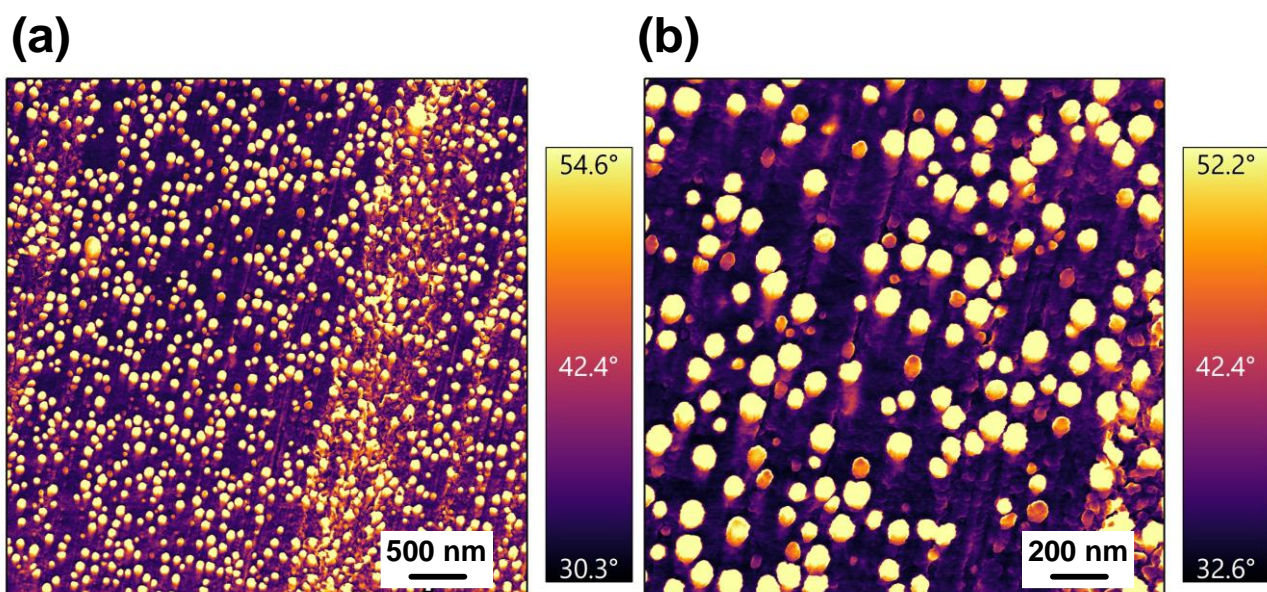


Figure S4. Atomic force microscopy (AFM) phase-contrast images of a neat epoxy matrix containing core–shell rubber (CSR) particles in the absence of silica fillers. Dispersed soft, rounded domains (light-colored regions with higher phase angles) with characteristic sizes of approximately 100–200 nm are observed, corresponding to nanoscale CSR domains within the rigid epoxy matrix (dark-colored regions with lower phase angles). (a) Image acquired over a scan area of $5 \times 5 \mu\text{m}^2$. (b) Image acquired over a scan area of $2 \times 2 \mu\text{m}^2$.

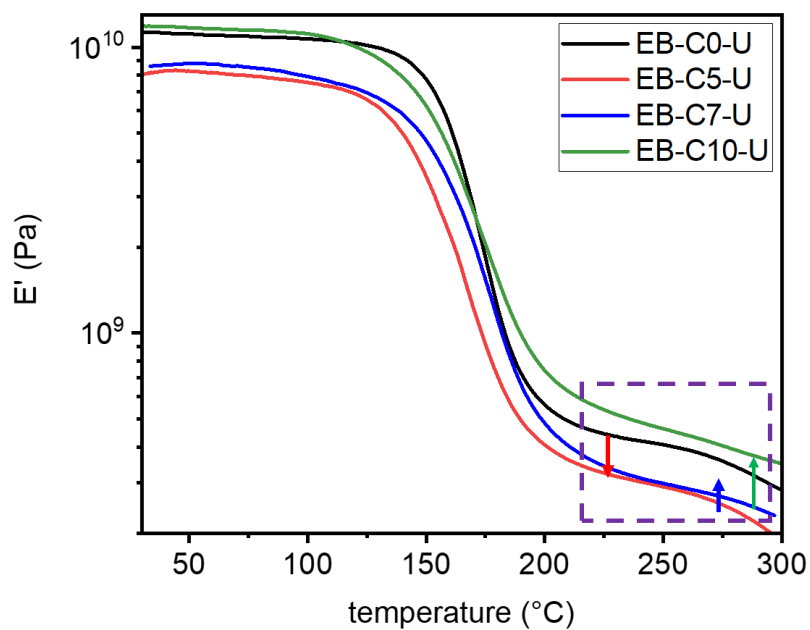


Figure S5. Temperature-dependent storage modulus (E') of the trimodal LMC systems with different CSR loadings. The purple-highlighted region emphasizes the rubbery-state modulus behavior at elevated temperatures, and the arrows indicate the anomalous modulus recovery observed with increasing CSR incorporation.

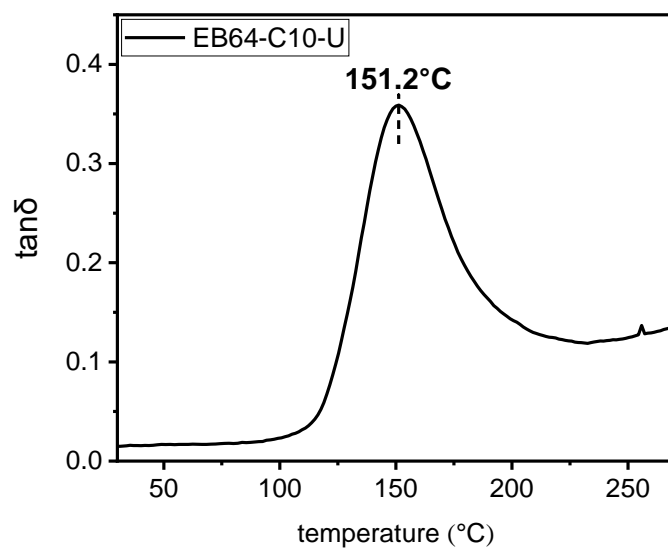


Figure S6. DMA tan δ -temperature curve of ECC:BDGE = 60:40 epoxy matrix, showing a Tg of ~ 150 $^{\circ}\text{C}$.

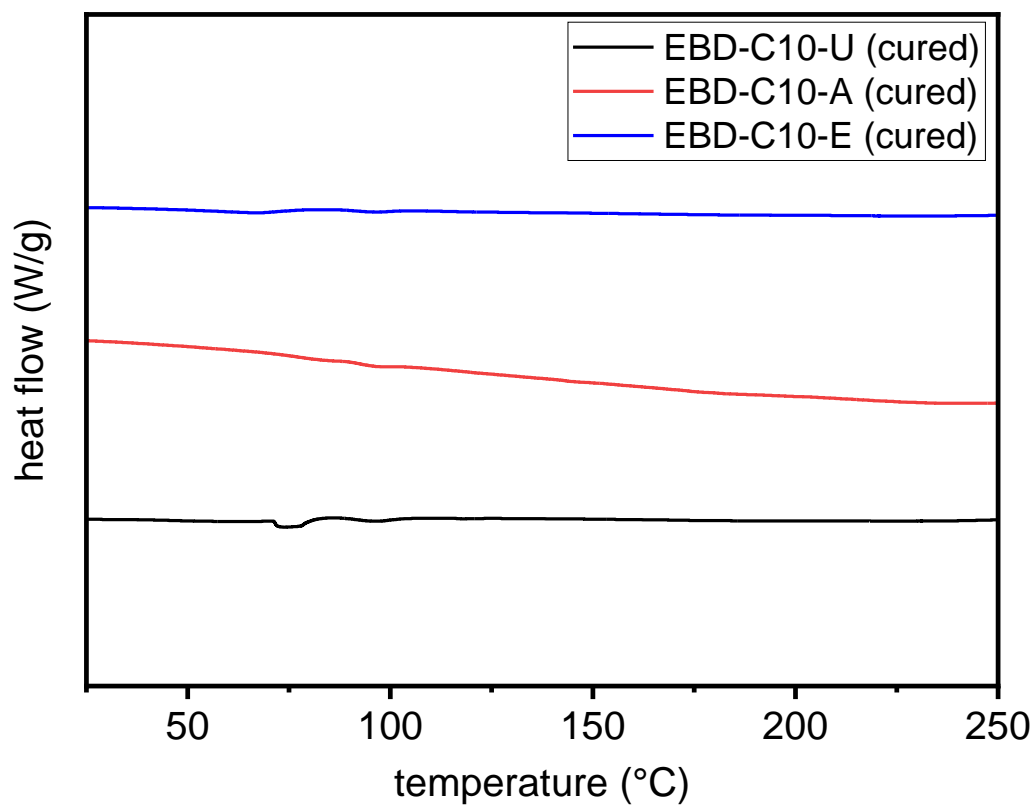


Figure S7. DSC thermograms of fully post-cured ternary LMC systems with different silica surface modifications (U, A, and E) after the rapid curing cycle (120 °C/5 min followed by 150 °C/1 h), showing no observable residual exothermic behavior.

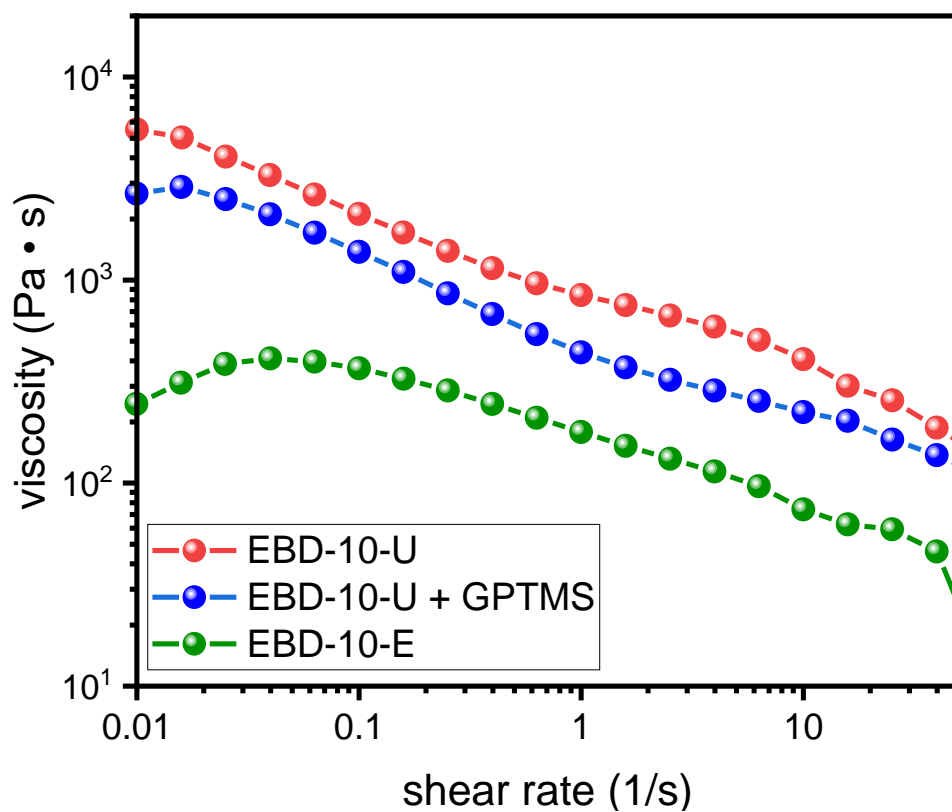


Figure S8. Viscosity–shear rate profiles of the epoxide-functionalized ternary LMC system (EBD-C10-E), the unmodified system (EBD-C10-U), and the physically mixed GPTMS control formulation containing non-covalent GPTMS (EBD-C10-U + GPTMS) at a loading comparable to the grafted organic content on the epoxide-functionalized silica (~0.33 wt%).

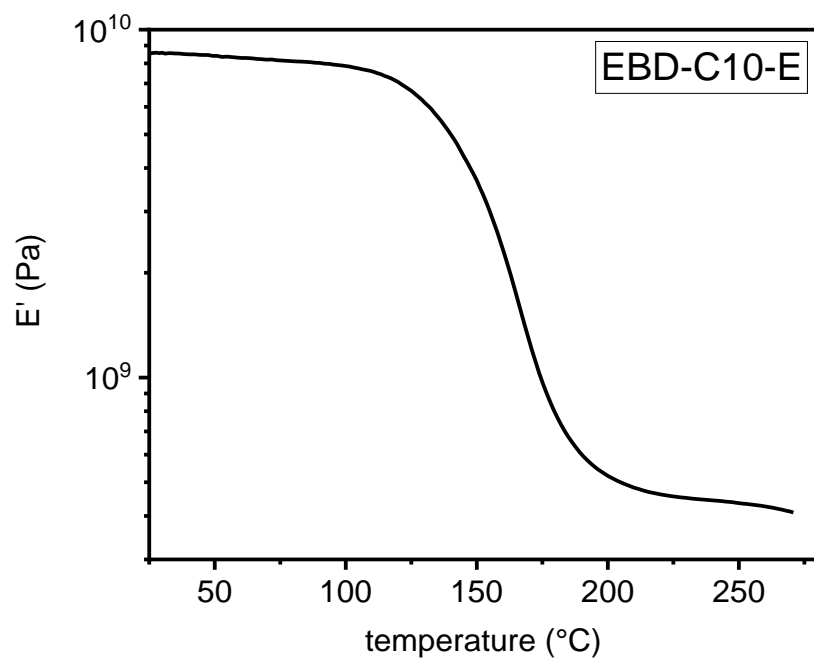


Figure S9. Temperature-dependent storage modulus (E') evolution of the optimized EBD-C10-E formulation, highlighting the progressive viscoelastic softening behavior across the thermomechanical transition region between the TMA- and DMA-derived T_g values.

Molded 6-inch wafer

Molded 4-inch wafer

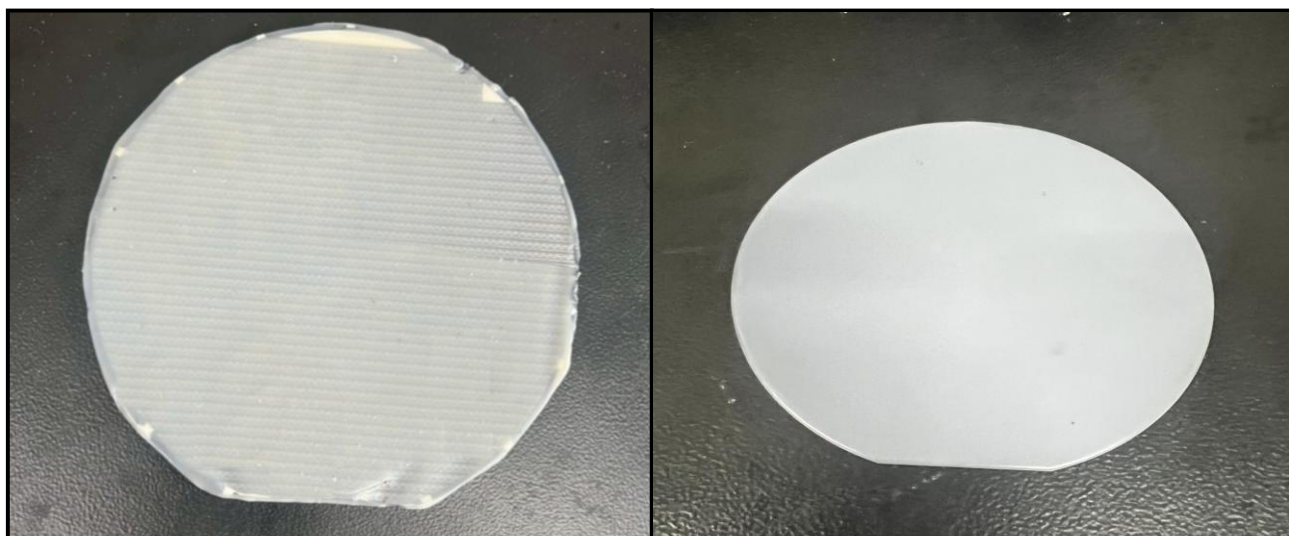


Figure S10. Surface photographs of 6-inch and 4-inch wafers molded with EBD-C10-E LMC, showing uniform replication and a defect-free appearance after compression molding.

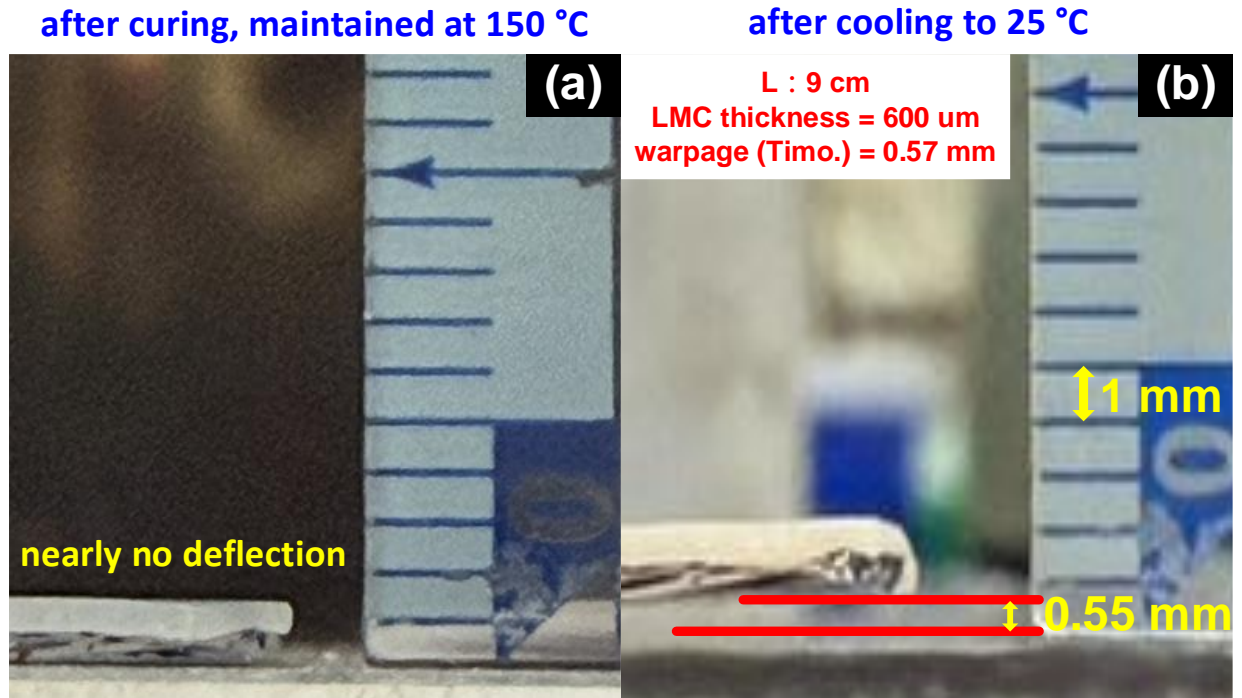


Figure S11. (a) LMC-molded strip sample maintained at 150 °C after the complete curing cycle (120 °C for 5 min followed by 150 °C for 1 h), showing negligible deflection. (b) Noticeable warpage developed after cooling to room temperature, with the measured deformation (~0.55 mm) in good agreement with the Timoshenko prediction (~0.57 mm).

ADDITIONAL TABLES

Table S1. Surface organic content and elemental ratios of coarse silica with different surface functionalities.

coarse silica type	unmodified	epoxide-modified	phenylamino-modified
organic content ¹	-	0.23 wt%	0.15 wt%
C/Si ratio ²	0.04	0.30	0.26
N/Si ratio ³	0.03	0.05	0.12

¹ The surface organic content was determined from TGA measurements of the silica samples. The residual weight loss of unmodified silica was used as the baseline, and the organic content was calculated by subtracting this baseline weight loss from that of the surface-modified samples.

^{2,3} The C/Si and N/Si ratios were calculated from EDS results as the atomic percentages of C and N normalized by the atomic percentage of Si.

Table S2. Estimated Hildebrand solubility parameters (δ) of epoxy monomers and anhydride curing agents used in the ternary curing system, calculated using the Fedors group contribution method.

component	ECC	BDGE	DGA	MHHPA	HHPA
δ ($MPa^{1/2}$) ¹	21.0	19.3	21.2	21.1	21.8

¹ The Hildebrand solubility parameter (δ) was estimated using the Fedors group contribution method, according to:

$$\delta = \left(\frac{\sum E_{coh}}{\sum V} \right)^{1/2}$$

where $\sum E_{coh}$ is the total cohesive energy contribution (J / mol) and $\sum V$ is the total molar volume contribution (cm^3 / mol) obtained from the Fedors group contribution constants.

Table S3. Property comparison of the present LMC with other highly filled epoxy molding compounds.

filler type	filler content	viscosity (Pa·s)*	α_1/α_2 (ppm/°C)	Tg (°C)	flexural strength (MPa)	reference
fused silica	40 vol%	5.7	18.1/50	~90 (DMA)	~100	[S1]
silica	50 vol%	-	~30/-	-	-	[S2]
silica	73 wt%	55	16.1/-	-	-	[S3]
AlN	65 vol%	solid type	14.5/-	~150 (TMA)	~180	[S4]
Al ₂ O ₃	90 wt%	~650	14.5/42	~240 (DMA)	-	[S5]
fused silica	87 wt%	~10 ⁴	11.5/21.5	147.4 (TMA)	142.2	[S6]
fused silica	87 wt% (78 vol%)	~250	8.2/22.5	172 (DMA) 156.4 (TMA)	~150	This work

*Viscosity values measured at ~20 rpm.

- S1. P. L. Teh, M. Jaafar, H. M. Akil, K. N. Seetharamu, A. N. R. Wagiman and K. S. Beh, *Polym. Adv. Technol.*, 2008, **19**, 308-315.
- S2. C. P. Wong and R. S. Bollampally, *Polym. Adv. Technol.*, 1999, **74**, 3396-3403.
- S3. Y. Ishikawa, T. Takao and T. Saito, *Microelectron. Reliab.*, 2023, **143**, 114933.
- S4. J.-W. Bae, W. Kim, S.-H. Cho and S.-H. Lee, *J. Mater. Sci.*, 2000, **35**, 5907-5913.
- S5. J. Li, B. Zhang, P. Zhu, G. Li, R. Sun and C. Wong, *2017 18th International Conference on Electronic Packaging Technology (ICEPT)*, 2017, 1107-1112.
- S6. W.-C. Chao, C.-P. Chu and Y.-C. Liao, *Compos. - A: Appl. Sci. Manuf.*, 2025, **192**, 108757.